FIRST ORDER OPTICAL MATCHING IN THE FINAL FOCUS SECTION OF THE SLAC LINEAR COLLIDER[*]

C.M. HAWKES

California Institute of Technology,
Pasadena, California 91125

and

P.S. BAMBADE

Stanford Linear Accelerator Center,
Stanford University, Stanford, California 94309

ABSTRACT

The procedures used for dispersion and betatron matching in the first order optical tuning of the SLC Final Focus are described. Associated modelling and fitting algorithms are presented.

A straightforward method for extending uncoupled optical models to incorporate cross-plane coupling is explained.

Submitted to *Nuclear Instruments and Methods* **A**

1. INTRODUCTION

The SLAC Linear Collider[1] (SLC) is designed to collide electron and positron bunches each with a round beam spot and with a transverse size of about 2 microns at the interaction point (IP). The Final Focus[2,3] sections of the beam lines, on each side of the IP, are responsible for focusing the beams to this small size.

The Final Focus optical system, shown in Fig. 1, consists of five telescopic modules. Demagnification is achieved in two stages, in the First and Final Telescopes. The chromaticity of the quadrupole array is compensated through sextupoles in the Chromatic Correction Section. Matching of the dispersion and the betatron motion to the Arc lattice is provided in the η-Matching Section and the First Telescope respectively. Extraction of the spent beam, moving in the opposite direction, is achieved in the First Telescope, through a pulsed magnet and a septum.

The Final Focus must also provide variable optical matching for the correction of distortions in the lattice arising through gradient errors in the beam line upstream and within the Final Focus Section itself. This note describes two parts of the optical tuning procedure used during the commissioning and running of the SLC Final Focus: the dispersion and betatron matching.

To attain the desired beam spot size, any contribution from the finite energy spread of the beam must be eliminated by making the beam dispersion zero at the IP. The method for doing this is described in Section 2.

The SLC design has equal emittances in the horizontal and vertical planes. In this case, six adjustments are involved to match the Final Focus monochromatic beam envelope to that coming out of the Arc. The procedure for doing this, referred to as betatron matching, is discussed in Section 3.

In order to perform these matching operations routinely it is necessary to have detailed optical modelling and fitting included as part of the online control

2

program for the Final Focus. The existing online SLC optical model was not adequate since it assumes that the beam dynamics in the horizontal and vertical planes are independent and hence cannot accommodate cross-plane coupling. A straightforward and general method for extending the model to incorporate cross-plane coupling was devised and is explained in Appendix A.

2. DISPERSION CORRECTION

2.1 DEFINITIONS

Dispersion refers to the correlation between the transverse position or angle of a particle in a bunch and its energy relative to the mean energy of the bunch; e.g. horizontal spatial dispersion:

$$\eta_x = \frac{\Delta x}{\delta} \tag{2.1}$$

where x is displacement in the local horizontal plane and δ is the energy spread, $\delta = \Delta E/E$. More precisely this can be termed the "beam dispersion". It corresponds to the sixth column of the beam σ-matrix[*] and contributes to the first-order transverse beam size according to the formula:

$$\sigma = \sqrt{\epsilon\beta + (\delta\eta)^2} \tag{2.2}$$

where ϵ is the emittance and $\sqrt{\epsilon\beta}$ is the monochromatic ($\delta = 0$) beam size.

The term "lattice dispersion" will be used to describe a slightly different quantity. It is a property of the optical lattice of the beam line, independent of the beam, and corresponds to the sixth column of the transfer matrix, or R-matrix,[*] describing a section of beam line. The lattice dispersion adds on to the

---

[*] The σ-matrix and R-matrix are defined in the manual for the program TRANSPORT.[4]

3

beam dispersion of a beam passing through the section; e.g. for horizontal spatial dispersion from point A to point B:

$$\eta_x^{\mathrm{B}} = R_{11}\eta_x^{\mathrm{A}} + R_{12}\eta_x'^{\mathrm{A}} + R_{13}\eta_y^{\mathrm{A}} + R_{14}\eta_y'^{\mathrm{A}} + R_{16} \qquad (2.3)$$

where η^{A} is the beam dispersion at the start of the section, η^{B} is the beam dispersion at the end of the section and R is the transfer matrix across the section. The horizontal spatial lattice dispersion from A to B is R_{16}.

2.2 DESIGN DISPERSION

The SLC requires zero spatial and angular beam dispersion (η and η') in x and y at the interaction point in order to optimise the luminosity. With an energy spread of 0.5% a residual spatial beam dispersion of only 1 mm will more than double the spot size from 2 to 5 microns.

Fig. 2 shows the design value for η_x as a function of distance along the beam line (z) in the Final Focus from the end of the Arc to the IP. Whereas η_y is designed to be zero everywhere in the Final Focus, this is not true of η_x. The condition $\eta_x^{\mathrm{IP}} = 0$ is achieved by having non-zero beam dispersion at the end of the Arc, $\eta_x^{\mathrm{ARC}} = 47.5\,\mathrm{mm}$. This is cancelled by an equal and opposite lattice dispersion in the η-Matching Section at the beginning of the Final Focus, leading to $\eta_x^{\mathrm{FT}} = 0$ at the end of the First Telescope (FT). The Chromatic Correction Section (CCS) temporarily generates large values of η_x as part of its function, but the design value of η_x returns to zero at the end of the CCS and through the Final Telescope to the IP.

4

2.3 ANOMALOUS DISPERSION

In practice the dispersion functions sometimes show anomalous deviations from the design. Possible errors contributing to a non-zero beam dispersion at the IP can be grouped into two classes.

(a) Beam dispersion coming from the Arc which is different from its design value.

(b) Anomalous dispersion arising from errors in elements of the Final Focus beam line itself. These are most likely to come from the CCS (due to misalignment of a sextupole or quadrupole, for example) since η_x is locally large there, and so small errors lead to big effects at the IP.

It is desirable to deal with errors of type (a) first by correcting the dispersion at the end of the First Telescope to give $\underline{\eta}^{\rm FT} = \underline{0}$.[*] If this anomalous dispersion is left uncorrected at the end of the FT it will propagate through to the IP. The Final Focus optics cause demagnification of the spatial dispersion component and magnification of the angular component. The resulting anomalous $\eta'^{\rm IP}$ is likely to be of much greater magnitude than $\eta^{\rm IP}$, making it difficult to measure $\eta^{\rm IP}$ accurately enough for it to be corrected at the IP.

Errors of type (b), combined with residual errors of type (a), must then be handled separately by correcting the dispersion at the IP to give $\underline{\eta}^{\rm IP} = \underline{0}$.

In both cases the tools available to make the dispersion correction are the same: two pairs of small quadrupoles in the η-Matching Section of the Final Focus with one upright and one skew quadrupole in each pair. These are shown cross-hatched in Fig. 1.[†] The skew quadrupoles, which are tilted at 45° to the standard axes, are needed to couple the non-zero x beam dispersion into the y plane and hence give some control over η_y. The pair CQ6 and SQ6 are approximately in

---

[*] The vector notation $\underline{\eta}$ will be used to represent all four components of η and η'.

[†] In Fig. 1 upright quadrupoles are represented by lens shapes and skew quadrupoles are represented by diamond shapes.

5

phase with the end of the FT whereas the pair CQ5 and SQ5 are approximately $\frac{\pi}{2}$ out of phase. The IP is in antiphase with the end of the FT. Hence, for a beam with design specifications coming from the Arc and with the correctors initially set to zero, the first pair controls η_x' and η_y' whereas the second pair controls η_x and η_y. This orthogonality is lost in moving away from the design parameters for the beam and lattice. However, it is always possible to find a combination of four quadrupole settings to correct the four $\underline{\eta}$ components at the end of the FT or at the IP. The only limitation is the maximum current available from the magnet power supplies.[*]

2.4   MEASURING DISPERSION

The spatial dispersion (η_x and η_y) at a point along the beam line can be measured by stepping the beam energy through, say, $\pm 0.3\%$ about its nominal value and finding the slope of a plot of displacement versus energy.[5] This can be done only at points where there is a device for measuring the transverse beam position, such as a beam position monitor (BPM) or, at the IP, a secondary emission wire target called the wire scanner.[6] This technique is illustrated in Fig. 3.

To infer the spatial and angular dispersion at any point a fit must be made to the η measurements. The details of this fitting procedure are given in Appendix B.

It should be noted that this technique in fact measures the *lattice* dispersion of the beam line between the point where the beam energy is varied (the Linac) and the location of the BPM. Any beam dispersion already in the Linac cannot be measured in this way. The design dispersion in the Linac is zero and any anomalous Linac dispersion is expected to be small. However, it will not be

---

[*] There are some values of $\underline{\eta}^{ARC}$ for which the effective range of the correctors becomes so small that the dispersion cannot be corrected using this scheme.[3] These "dead zones" can be avoided by adjusting the dispersion upstream.

measured and hence will not be corrected by the First Telescope Dispersion Correction scheme to be described in Section 2.5. It will propagate through to the IP and must be corrected there as described in Section 2.6.

2.5 FIRST TELESCOPE DISPERSION CORRECTION

To correct the dispersion at the end of the First Telescope it is first necessary to determine the spatial and angular dispersion at the end of the Arc, $\underline{\eta}^{\text{ARC}}$. This is done by measuring the spatial dispersion at BPMs near the end of the Arc, as described in Section 2.4, and then using the fitting technique described in Appendix B.

The model is used to transport $\underline{\eta}^{\text{ARC}}$ through the η-Matching and FT Sections of the Final Focus to give $\underline{\eta}^{\text{FT}}$ at the end of the FT:

$$\underline{\eta}^{\text{FT}} = R^{\text{ARC}\rightarrow\text{FT}}(k_1, k_2, k_3, k_4)\, \underline{\eta}^{\text{ARC}} \tag{2.4}$$

where, now,

$$\underline{\eta}^{\text{ARC}} = \left(\eta_x^{\text{ARC}}, \eta_x'^{\text{ARC}}, \eta_y^{\text{ARC}}, \eta_y'^{\text{ARC}}, 0, 1 \right) \tag{2.5}$$

$$\underline{\eta}^{\text{FT}} = \left(\eta_x^{\text{FT}}, \eta_x'^{\text{FT}}, \eta_y^{\text{FT}}, \eta_y'^{\text{FT}}, 0, 1 \right) \tag{2.6}$$

and $R^{\text{ARC}\rightarrow\text{FT}}$ is the transfer matrix from the end of the Arc to the end of the FT calculated from the model. The sixth element of the $\underline{\eta}$ vectors, which is always unity, ensures that the lattice dispersion elements contained in the final column of R are correctly incorporated according to equation (2.3).

The matrix, $R^{\text{ARC}\rightarrow\text{FT}}$, is a function of k_1, k_2, k_3 and k_4, the magnetic strengths of the four dispersion corrector quadrupoles described above. In order to make $\underline{\eta}^{\text{FT}} = \underline{0}$, the values of k_1, k_2, k_3, k_4 must be found which minimise $\underline{\eta}^{\text{FT}}$. This is done using the least squares fitting program, NPSLAC.[7]   The

7

corrector strengths are varied and $R^{\mathrm{ARC \to FT}}$ and $\underline{\eta}^{\mathrm{FT}}$ evaluated for each new set of strengths. The minimisation program exits when the sum

$$\sum_{i=1}^{4} \left\{ \eta_i^{\mathrm{FT}} \right\}^2 \tag{2.7}$$

is sufficiently small. The corresponding values of k_1, k_2, k_3, k_4 are returned and can be used to set the strengths of the physical magnets.

This algorithm was used regularly during the 1987 period of the SLC Final Focus commissioning[8] and has now become routine and highly reliable. Correction usually yields a dispersion function within a few per cent of the design. One example is shown in Fig. 4. Up to now, the ultimate limit to the precision of this correction has been small alignment errors on the dispersion correction quadrupoles themselves. As their strengths are varied to perform the correction, the misalignment causes the beam to be steered as well as focused downstream and hence the result is not exactly as predicted by the online model.

2.6   INTERACTION POINT DISPERSION CORRECTION

Even after a successful $\underline{\eta}^{\mathrm{FT}}$ correction there might still be beam dispersion at the IP which must be corrected. This can be due to residual anomalous dispersion propagating from the FT or due to alignment or magnetic errors in the Final Focus beam line itself.

One possible technique is to determine $\underline{\eta}^{\mathrm{IP}}$ using the wire scanner and the BPMs near to the IP and the measurement and fitting schemes described in Section 2.4 and Appendix B. Corrector settings can then be calculated which will generate an equal and opposite $-\underline{\eta}^{\mathrm{IP}}$. On iteration the IP dispersion should tend towards zero. There are two disadvantages to this method. Firstly it requires an accurate measurement of $\underline{\eta}^{\mathrm{IP}}$. As explained in Section 2.4 this is difficult because of the spatial demagnification produced by the Final Focus. Secondly, the measurement technique of Section 2.4 is insensitive to anomalous dispersion

generated in the Linac or further upstream, since it actually measures the lattice dispersion between the point where the beam energy is varied and the measurement device. Hence this contribution to the beam dispersion at the IP would not be corrected.

Another technique involves minimising the true beam dispersion at the IP by using the transverse beam spot size as measured by the wire scanner.[6] The spot size is directly related to the beam dispersion according to equation (2.2). For each of the four components of $\underline{\eta}^{\mathrm{IP}}$, four coefficients are found corresponding to the changes in each of the four corrector quadrupole settings needed to produce a unit change in that component of $\underline{\eta}^{\mathrm{IP}}$ while leaving the other three components of $\underline{\eta}^{\mathrm{IP}}$ unchanged. These represent orthogonal "η-knobs" for controlling the dispersion at the IP.* A scan can then be made over a suitable range of each component of $\underline{\eta}^{\mathrm{IP}}$ and the size of the spot at the IP measured at each point in the scan. To first order, the minimum spot size corresponds to the optimum corrector settings.

3. BETATRON MATCHING

3.1   BETATRON PHASE-SPACE DISTORTIONS

The six distortions of the betatron phase-space which are possible[3] in the case of equal horizontal and vertical emittances are the two waist offsets ($< x\theta >$ and $< y\phi >$ correlations), the two IP angular spreads and two cross-plane correlations of IP angles ($< \theta\phi >$) and of IP positions to angles ($< x\phi >$).

★ In fact the problem is nonlinear. Adjustments to upstream corrector quadrupoles change the dispersion of the beam passing through downstream correctors, and hence they cannot be decoupled completely. However, over a limited range of $\underline{\eta}^{\mathrm{IP}}$ a linear approximation is valid.

If the Final Focus optics has been changed from the design configuration of $\beta^* = 7.5\,\mathrm{mm}$ (see Section 3.2) then these "η-knobs" will also move the positions of the beam waists along z away from the IP ($\alpha \neq 0$). Additional corrections must be made to compensate for this effect.

The angular spread terms are controlled upstream of the CCS by cancelling the $< \theta\phi >$ cross term with a skew quadrupole (SQ17.5) and by varying β^* in each plane with two quadrupoles (16 and 17). This amounts to detuning the overall demagnification factor in the Final Focus beam line. Waist terms are corrected at the very end, with trim windings on the last quadrupoles (2B and 3) and another skew quadrupole (SQ3) immediately upstream. Two additional terms ($< xy >$ and $< y\theta >$) would require additional correction elements in the case of unequal emittances, but are redundant otherwise. All six quadrupoles which must be controlled to achieve this are shaded in Fig. 1.

The waists must be positioned at the collision point to within the depth of field $\beta^* \simeq 1\,\text{cm}$ and the $< x\phi >$ correlation removed.

After cancelling the $< \theta\phi >$ cross-term, β^*, which for fixed emittance determines the angular spread, must[3] be adjusted close to the design optimum. This optimum occurs when linear optics and higher order effects contribute about equally to the spot size at the waist. For β^* too small, the IP spot is dominated by chromatic aberrations (third order if the second order chromatic correction is properly tuned, second and third order otherwise). Conversely for β^* too large, it is dominated by a larger linear size. The tolerance[3] on β^* is about 50%.

3.2 CORRECTION PROCEDURE

Waist controls can be made orthogonal, linear and independent of input phase-space distortions, allowing position to angle correlations in the IP spot to be cancelled by empirically minimising its size. This is done using the wire scanner.[6] Spots are measured as functions of the orthogonal waist controls, and a parabola, $\epsilon\beta^* + \epsilon/\beta^* \Delta f^2$, is fitted to the square of the spot size (where Δf is the distance to the waist) to determine both ϵ and β^*.

Actual angular spreads are well determined from the branches of the parabola, but both ϵ and β^* estimates suffer if the linear spot is not resolved. This can arise through residual cross-plane coupling, only partially corrected in cases of

unequal emittances, and through third order chromatic aberration which can dominate before the betatron matching is fully implemented. Sextupoles must also be fitted in the perturbed lattice at each iteration of the betatron matching procedure described here, to preserve good second order correction.

Measured values of β^* are used to determine angular corrections needed for matching. The adjustments are nonlinear functions of the three quadrupoles used for control. In addition, the correctors also affect the waists. The solution must therefore be the result of an overall fit of the six correctors towards the desired IP phase-space. The fitting procedure is outlined in Section 3.3. Because of the uncertainty in the measurement noted above, some amount of guessing is also necessary to determine the matching correction required. The procedure must in general be iterated in an empirical search for the optimal angular correction.

The online modelling and fitting package developed allows full flexibility in the generation of detuned optical configurations needed to match distorted beam envelopes, based on measured or on estimated optical parameters. The fitting procedure can also be adjusted conveniently by user intervention, to suit specific situations. This is explained in more detail in Appendix C. An example of such a detuned solution is shown in Fig. 2. The solid β_x and β_y curves show the design lattice of $\beta^* = 7.5$ mm. The dash-dotted curves show a detuned configuration calculated to give $\beta^* = 30$ mm. This lattice is presently installed as the default configuration for commissioning of the SLC. It corresponds to a first guess of the most probable angular correction needed to match possibly varying optical mismatch at the Final Focus input, generated by errors and tuning in the upstream systems. In this configuration, residual angular errors are small enough to reproduce small IP spots at the five micron level by sweeping *only* the three waist controls. It is anticipated that additional iterations of this matching will be required to optimise the spot size further.

3.3 FITTING PROCEDURE

Before starting the last stage of betatron matching it is assumed that, to a first approximation, the dispersion has been corrected as described in Section 2, and the waist and cross-plane coupling corrections have been completed as outlined in Section 3.2. Hence α_x, α_y and all the cross-plane terms in the beam σ-matrix[*] at the IP are approximately zero. The assumed initial σ-matrix ("0th iteration") is:

$$\sigma^{\text{IP}}(0) = \begin{pmatrix} \beta_x^*(0)\epsilon_x & 0 & 0 & 0 \\ 0 & \epsilon_x/\beta_x^*(0) & 0 & 0 \\ 0 & 0 & \beta_y^*(0)\epsilon_y & 0 \\ 0 & 0 & 0 & \epsilon_y/\beta_y^*(0) \end{pmatrix} \qquad (3.1)$$

It is diagonal and can be specified by four independent parameters. Any two out of σ_x^* (spatial size at IP $= \sqrt{\sigma_{11}}$), $\sigma_x'^*$ (angular size at IP $= \sqrt{\sigma_{22}}$), ϵ_x (emittance) and β_x^* (betatron function at IP) can be measured to determine the initial σ_x^{IP} matrix, and similarly for y.

The σ matrix of the beam at the end of the Arc is then:

$$\sigma^{\text{ARC}} = R^{-1}(\underline{k}(0)) \cdot \sigma^{\text{IP}}(0) \cdot \left[R^{-1}(\underline{k}(0))\right]^{\text{T}} \qquad (3.2)$$

where $R(\underline{k}(0))$ is the initial transfer matrix from the end of the Arc to the IP and

$$\underline{k}(0) = k_1(0), k_2(0), \ldots, k_{\text{n}}(0) \qquad (3.3)$$

are the initial strengths of the n quadrupoles and skew quadrupoles in the Final Focus beam line which are used for the betatron matching.

---

[*] The notation used for σ-matrix elements is the same as that described on pages 33-35 of the TRANSPORT manual.[4] For simplicity, only the first four columns and rows of the σ-matrix are shown.

The goal after the 1ˢᵗ iteration of betatron matching is to find a new set of strengths, $\underline{k}(1)$, such that:

$$\sigma^{\mathrm{IP}}(1) = R(\underline{k}(1)) \cdot \sigma^{\mathrm{ARC}} \cdot [R(\underline{k}(1))]^{\mathrm{T}}$$

$$= \begin{pmatrix} \beta_x^*(1)\epsilon_x & 0 & 0 & 0 \\ 0 & \epsilon_x/\beta_x^*(1) & 0 & 0 \\ 0 & 0 & \beta_y^*(1)\epsilon_y & 0 \\ 0 & 0 & 0 & \epsilon_y/\beta_y^*(1) \end{pmatrix} \qquad (3.4)$$

is the desired σ-matrix at the IP. To go from equation (3.1) to (3.4) the spatial magnification is changed by a factor of $\sqrt{\beta^*(1)/\beta^*(0)}$ (which may be different in x and y), while the off-diagonal terms (α_x, α_y and cross-plane coupling) are kept at zero. The details of the fitting algorithm used are presented in Appendix C. The quadrupole strengths, $\underline{k}(1)$, returned by the fitter after the first iteration can be used to set the physical magnets on the beam line.

The beam spot is then remeasured and further iterations of the matching procedure are implemented to optimise the luminosity.

One example of a small spot measured during the 1987 SLC commissioning is shown in Fig. 5. At the time of writing the smallest electron spot sizes which have so far been obtained were measured at 3-4 microns. Simultaneous electron and positron spot sizes of 5-7 microns can be reproduced without difficulty. Commissioning work is continuing to bring the SLC parameters up to the level necessary for the production of Z^0 events.

APPENDIX A

MODELLING CROSS-PLANE COUPLING

A1 TWISS PARAMETERS

In the SLC control program[9] the standard online optical model of the machine[10] is stored in the form of so-called Twiss parameters at each significant point along the beam line:

ψ_x = the horizontal betatron phase or tune (sometimes denoted by ν_x)

β_x = the horizontal betatron function

α_x = the horizontal alpha function

η_x = the horizontal spatial dispersion

η'_x = the horizontal angular dispersion

and similarly in the vertical (y) direction. The Twiss parameters are generated by running the program COMFORT (Version 3),[11] using as input either design parameters or values taken from the SLC online database.[10,9]

In order to model a section of the beam line between points A and B it is necessary to know the 6×6 first order beam transfer matrix,[*] R, from A to B. If the optics in x and y planes are independent then it can be written in the form:

$$R = \begin{pmatrix} R_{11} & R_{12} & 0 & 0 & 0 & R_{16} \\ R_{21} & R_{22} & 0 & 0 & 0 & R_{26} \\ 0 & 0 & R_{33} & R_{34} & 0 & R_{36} \\ 0 & 0 & R_{43} & R_{44} & 0 & R_{46} \\ 0 & 0 & 0 & 0 & 1 & 0 \\ 0 & 0 & 0 & 0 & 0 & 1 \end{pmatrix} \qquad \text{(A1)}$$

with all cross-plane coupling elements at zero.

---

[*] The notation used for transfer matrix elements is that described on pages 4 and 5 of the TRANSPORT manual.[4]

In this case the elements of R can be evaluated from the Twiss parameters at points A and B using standard formulae. For x:

$$R_{11} = \sqrt{\beta_B/\beta_A}(\cos \Delta\psi + \alpha_A \sin \Delta\psi)$$
$$R_{12} = \sqrt{\beta_A\beta_B} \sin \Delta\psi$$
$$R_{16} = \eta_B - R_{11}\eta_A - R_{12}\eta'_A$$
$$R_{21} = -\{(1 + \alpha_A\alpha_B) \sin \Delta\psi + (\alpha_B - \alpha_A) \cos \Delta\psi\}/\sqrt{\beta_A\beta_B} \qquad (A2)$$
$$R_{22} = \sqrt{\beta_A/\beta_B}(\cos \Delta\psi - \alpha_B \sin \Delta\psi)$$
$$R_{26} = \eta'_B - R_{21}\eta_A - R_{22}\eta'_A$$

where $\qquad \Delta\psi = \psi_B - \psi_A$

For y, these formulae give R_{33}, R_{34}, R_{36}, R_{43}, R_{44} and R_{46} respectively. To obtain the transfer matrix elements only the change in the Twiss parameters between points A and B is needed. Their absolute values at each point are not important for this purpose.

A2   CROSS-PLANE COUPLING

The procedure outlined in Section A1 is valid only if there is no coupling between x and y planes since the x and y Twiss parameters are assumed to be independent. That is, it works only if the transfer matrix can be written in the form of equation (A1).

This is a valid representation for most standard beam line elements, but it is invalid for skew quadrupoles and rotations of the coordinate system (rolls). Since skew quadrupoles play a vital part in the SLC Final Focus optics it was necessary to modify the online modelling.

One solution would be to abandon the present model and replace it with one where the full two-dimensional transfer matrix to each beam line point is stored.

Since COMFORT (Version 3)[11] does not include cross-plane coupling this would also need to be upgraded.†

Instead it was decided to keep the Twiss parameters and to add a relatively small amount of extra dedicated Final Focus modelling and fitting code to handle cross-plane coupling where this was necessary. To do this the model beam line is divided into a series of discrete, sequential sections of two sorts:

(a) those for which cross-plane coupling is unimportant, i.e. there are no skew quadrupoles, rolls or similar beam line elements;

(b) those for which cross-plane coupling is important.

For category (a) the online Twiss parameters for the points at the beginning and end of the section are sufficient. The full two-dimensional transfer matrix can be found using equations (A2) and (A1).

For category (b) the Twiss parameters cannot be used. However, these sections can be reduced so that they consist of just a single beam line element – a single skew quadrupole or a roll, for example. In these cases the full two-dimensional transfer matrix can be determined separately using a small number of input parameters taken from the online database. In the case of a skew quadrupole the data required are the integrated magnetic field gradient (strength), the effective length of the magnet, the skew angle and the energy and charge of the beam.

Thus a set of consecutive transfer matrices is produced, running between each of the points along the whole beam line. By multiplying this string of matrices together in the correct sequence the cumulative transfer matrix between any two of the points can be obtained. This is all that is needed for a model incorporating cross-plane coupling.

It is sometimes useful to enlarge category (b) above. For example, to perform a fit in which the magnetic strengths of certain quadrupoles are allowed to vary

---

† When COMFORT is used to generate Twiss parameters for the present online model rolls are ignored and skew quadrupoles are treated as drift spaces.

in the model, each of these quadrupoles is treated as a separate beam line section. After each iteration of the fit, their transfer matrices are recalculated using the new magnetic strengths and hence the cumulative transfer matrix for the whole beam line is updated. This technique is used in the programs for the dispersion and betatron matching which are described in the main text.

APPENDIX B

DETERMINATION OF SPATIAL AND ANGULAR DISPERSION

This Appendix describes the fitting technique used to determine the spatial and angular dispersion at any point P from spatial dispersion measurements made by beam position monitors.

Measure η_x^i and η_y^i, $i = 1, N$, the spatial dispersions in x and y at N points. Using a model of the beam line, as explained in Appendix A, evaluate the transfer matrices, R^i, between P and each of the measurement points. From the first and third rows of each transfer matrix a new matrix, A, of dimensions $4 \times 2N$, can be formed, which relates the spatial and angular dispersions at the point P to the spatial dispersion measurements:-

$$\Delta \underline{\eta} = A \, \underline{\eta}^P \tag{B1}$$

where

$$\Delta \underline{\eta} = \left(\eta_x^1 - R_{16}^1, \eta_y^1 - R_{36}^1, \eta_x^2 - R_{16}^2, \ldots, \eta_x^N - R_{16}^N, \eta_y^N - R_{36}^N \right) \tag{B2}$$

$$\underline{\eta}^P = \left(\eta_x^P, {\eta_x'}^P, \eta_y^P, {\eta_y'}^P \right) \tag{B3}$$

17

and the rows of A are formed from the rows of R^i by (j=1,4):

$$A_{1j} = R^1_{1j}$$

$$A_{2j} = R^1_{3j}$$

$$A_{3j} = R^2_{1j}$$

$$\vdots$$

$$A_{(2N-1)j} = R^N_{1j}$$

$$A_{2Nj} = R^N_{3j}$$

(B4)

The R_{16} (R_{36}) elements are subtracted from the η_x (η_y) measurements in order to eliminate the lattice dispersion component which the model associates with the beam line between P and the measurement points. The remainder, $\Delta\underline{\eta}$, is the spatial dispersion at the points associated solely with the dispersion at P.

In order to solve for $\underline{\eta}^P$ the matrix equation (B1) must be inverted. Since A is not a square matrix the solution is not unique. The estimated uncertainties, σ_i, on the η_i measurements can be used as weighting factors to obtain a unique inversion. The χ^2 sum:-

$$\sum_{i=1}^{2N} \left\{ \frac{\left(\sum_{j=1}^{4} A_{ij}\eta_j^P \right) - \Delta\eta_i}{\sigma_i} \right\}^2$$

(B5)

is minimised by taking

$$\underline{\eta}^P = (BA)^{-1} B \,\Delta\underline{\eta}$$

(B6)

where the elements of the $2N \times 4$ dimensional matrix B are formed from those of A by

$$B_{ji} = \frac{A_{ij}}{\sigma_i^2}$$

(B7)

Hence the spatial and angular dispersions at P can be inferred from the measurements.

APPENDIX C

FITTING ALGORITHM FOR BETATRON MATCHING

The details of the fitting algorithm used for the betatron matching scheme described in Section 3.3 are presented in this Appendix.

The least squares fitting program NPSLAC[7] is used. The strengths, $\underline{k}$, of all the quadrupoles to be used for the betatron matching are varied and $R(\underline{k})$, the transfer matrix from the end of the Arc to the IP, and σ^{IP}, the beam σ-matrix at the IP, are evaluated for each new set. The program minimises a sum of squares composed from the elements of σ^{IP}:

$$(\beta_x \text{ term})^2 + (\beta_y \text{ term})^2 + \left(\frac{\sigma_{12}}{\sqrt{\sigma_{11}\sigma_{22}}}\right)^2 + \left(\frac{\sigma_{34}}{\sqrt{\sigma_{33}\sigma_{44}}}\right)^2$$

$$+ \left(\frac{\sigma_{13}}{\sqrt{\sigma_{11}\sigma_{33}}}\right)^2 + \left(\frac{\sigma_{24}}{\sqrt{\sigma_{22}\sigma_{44}}}\right)^2 + \left(\frac{\sigma_{23}}{\sqrt{\sigma_{22}\sigma_{33}}}\right)^2 + \left(\frac{\sigma_{14}}{\sqrt{\sigma_{11}\sigma_{44}}}\right)^2 \qquad \text{(C1)}$$

Depending on the input beam parameters some of these terms may be omitted from the sum so that those σ-elements remain free.

The third and fourth terms of this sum constrain α_x and α_y to remain at zero and hence keep the beam waists at the IP. The last four terms keep all cross-plane coupling terms at zero. The denominators make each term a dimensionless and reasonably scaled number.

Studies using offline simulations[12,3] have shown that different expressions are needed for the "β_x term" and "β_y term" depending on the initial input, in order to ensure that the fit converges rapidly and reliably. For many input conditions, using:

$$\beta_x \text{ term} = \frac{\sigma_{22} - \epsilon_x/\beta_x^*(1)}{\epsilon_x/\beta_x^*(1)} \qquad \text{(C2)}$$

(similarly for β_y) is found to give satisfactory results. This is equivalent to fitting

the angular beam size. Sometimes it is better to fit the spatial beam size:

$$\beta_x \text{ term} = \frac{\sigma_{11} - \beta_x^*(1)\epsilon_x}{\beta_x^*(1)\epsilon_x} \tag{C3}$$

or sometimes spatial and angular sizes together.

For both cases (C2) and (C3) it is necessary to constrain the R_{22} and R_{44} elements of the transfer matrix between the end of the Arc and the IP to remain less than zero. This ensures that the fit converges to the correct minimum.[*] For difficult situations, such as having unequal emittances in x and y, it is sometimes better to fit these elements directly:

$$\beta_x \text{ term} = \frac{R_{22} - R_{22}(\text{fit})}{R_{22}(\text{fit})} \tag{C4}$$

where $R_{22}(\text{fit}) = R_{22}(\underline{k}(0))\sqrt{\beta_x^*(0)/\beta_x^*(1)}$.

The efficiency and resilience of the fitting program can also be improved by splitting the minimisation up into several steps. The output from step number n is used as the input to step number n+1. The steps are chosen to guide the fitter along a path which is known to lead towards the desired minimum, taking into account the properties of the optics of the Final Focus beam line. For a range of input conditions the following two-step fit is found to be suitable:

(a) Fit β_x, β_y and minimise σ_{13}, leaving other σ-elements free. Only two upright quadrupoles (17 and 16) and the nearby skew quadrupole (SQ17.5) are allowed to vary in the fit, all others having their strengths fixed. These quadrupoles are in the First Telescope and are the ones most sensitive to β_x, β_y and σ_{13}. Quadrupoles 17 and 16 control the overall demagnification factor of the Final Focus and are the ones whose strengths are changed most during the betatron matching.

---

[*] A solution with R_{22} or R_{44} greater than zero corresponds to having an extra beam waist, in x or y, upstream from the IP.

(b) Minimise α_x, α_y and σ_{23} while keeping β_x, β_y and σ_{13} at the values they have after step (a). In addition to the three quadrupoles varied during step (a), two more upright quadrupoles (3 and 2B) and the nearby skew quadrupole (SQ3) are also allowed to vary. These are in the Final Telescope. Step (b) amounts to a minor retuning of the optics to reposition the horizontal and vertical beam waists at the IP ($\alpha = 0$) and eliminate remaining cross-plane coupling.

This two-step fit is the default used in the SLC control program, but great flexibility is available for changing the fitting algorithm when necessary.

ACKNOWLEDGEMENTS

REFERENCES

1. SLC Design Handbook, SLAC (December 1984)

2. Roger A. Erickson: Final Focus Systems for Linear Colliders, U.S. Summer School on High Energy Particle Accelerators (Batavia, Illinois; August 1984). SLAC-PUB-4479 (November 1987)
   J.J. Murray, K.L. Brown, T. Fieguth: The Completed Design of the SLC Final Focus System, Particle Accelerator Conference (Washington, DC; March 1987). SLAC-PUB-4219 (February 1987)
   Karl L. Brown: A Conceptual Design of Final Focus Systems for Linear Colliders, Joint US-CERN School on Particle Accelerators (South Padre, Texas; October 1986). SLAC-PUB-4159 (June 1987)

3. P.S. Bambade: Beam Dynamics in the SLC Final Focus System, Particle Accelerator Conference (Washington, DC; March 1987). SLAC-PUB-4227 (June 1987)

4. K.L. Brown, F. Rothacker, D.C. Carey, Ch. Iselin: TRANSPORT – A Computer Program for Designing Charged Particle Beam Transport Systems, SLAC-91, Rev. 2 (May 1977)

5. Miguel Flores: Correlation Plots Dispersion Function Measurement Utility (February 1987), unpublished

6. C. Field et al: A High Resolution Wire Scanner for Micron-Size Profile Measurements at the SLC, to be published. SLAC-PUB-4605 (April 1988)

7. NPSLAC is a modified version of the fitting package, NPSOL: Philip E. Gill, Walter Murray, Michael A. Saunders, Margaret H. Wright: User's Guide for NPSOL (Version 4.0): A Fortran Package for Nonlinear Programming, Technical Report SOL 86-2, Systems Optimization Laboratory, Stanford, CA 94305 (January 1986)
   Differences between NPSOL and NPSLAC are discussed in an internal

SLAC Single Pass Collider Memo: Chris Hawkes, Martin Lee: Recent Upgrading of the Modelling Program COMFORT, CN-342 (September 1986)

8. W. Kozanecki: Progress Report on the SLAC Linear Collider, International Europhysics Conference on High Energy Physics (Uppsala, Sweden; June-July 1987). SLAC-PUB-4465 (November 1987)

9. N. Phinney, H. Shoaee: The SLC Control System – Status and Development, Particle Accelerator Conference (Washington, DC; March 1987). SLAC-PUB-4215 (March 1987)
   N. Phinney: Report on the SLC Control System, IEEE Trans. Nucl. Sci., NS-32 no. 5, 2117 (1985). SLAC-PUB-3668 (May 1985)
   R.E. Melen: Design and Performance of the Stanford Linear Collider Control System, IEEE Trans. Nucl. Sci., NS-32 no. 1, 230 (1985). SLAC-PUB-3467 (October 1984)

10. M.D. Woodley, L. Sanchez-Chopitea, H. Shoaee: Application of Online Modeling to the Operation of SLC, Particle Accelerator Conference (Washington, DC; March 1987). SLAC-PUB-4249 (February 1987)
    J.C. Sheppard, R.H. Helm, M.J. Lee, M.D. Woodley: On-Line Control Models for the Stanford Linear Collider, IEEE Trans. Nucl. Sci., NS-30 no. 4, 2320 (1983). SLAC-PUB-3072 (March 1983)

11. L. Sanchez, H. Shoaee, M. Woodley: COMFORT – Control of Machine Functions, Orbits, and Trajectories, Version 3.0, SLAC (March 1986), unpublished
    M.D. Woodley, M.J. Lee, J. Jäger, A.S. King: Control of Machine Functions or Transport Systems, IEEE Trans. Nucl. Sci., NS-30 no. 4, 2367 (1983). SLAC-PUB-3086 (March 1983)
    See also Ref. 10.

12. W. Kozanecki: private communication

FIGURE CAPTIONS

1. The optical design of the SLC Final Focus. The four quadrupoles used for the dispersion correction are shown cross-hatched and the six quadrupoles used for betatron matching are shown shaded.

2. Betatron and dispersion functions of the SLC Final Focus. The η_y function (not shown) is zero everywhere. The solid curves show the SLC design whereas the dash-dotted curves show β_x and β_y in the detuned $\beta^* = 30\,\mathrm{mm}$ configuration described in Section 3.2 of the main text.

3. Dispersion Measurement Technique. To measure the lattice dispersion of a section of beam line from A to B (here represented as a single bend magnet) the beam energy is increased from E to $E + \Delta E$ and the beam deflection at point B, Δx, is measured using a BPM. The dispersion is $\Delta x/(\Delta E/E)$. If the beam dispersion at A is zero then this is a measure of η_x^{B}, the beam dispersion at B. In practice the dispersion is obtained by averaging over a scan of several different beam energies, and at each energy point Δx is measured by taking the average of several BPM readings on successive beam pulses.

4. The First Telescope Dispersion Correction. The horizontal (upper figures) and vertical (lower figures) dispersion is shown before (left) and after (right) correction, using an example of data taken during the 1987 SLC commissioning. Note the changes in scale. In each figure the error bars on the solid curve show the results of simultaneous dispersion measurements on the electron beam using BPMs in the SLC North Arc and the η-Matching, First Telescope and Chromatic Correction Sections of the North Final Focus. The solid curve is a series of straight lines joining these measurement points. The dotted curve is a series of straight lines joining points showing the corresponding value of the design dispersion at the location of each of the BPMs. After correction the measured dispersion in the η-Matching and First Telescope Sections is very close to the design values.

5. An example of a transverse scan of the electron beam at the Interaction Point, using wire scanner data from the 1987 SLC commissioning. Unfolding the 3.5 micron size of the wire target gives a corrected beam size of 4.6 microns.
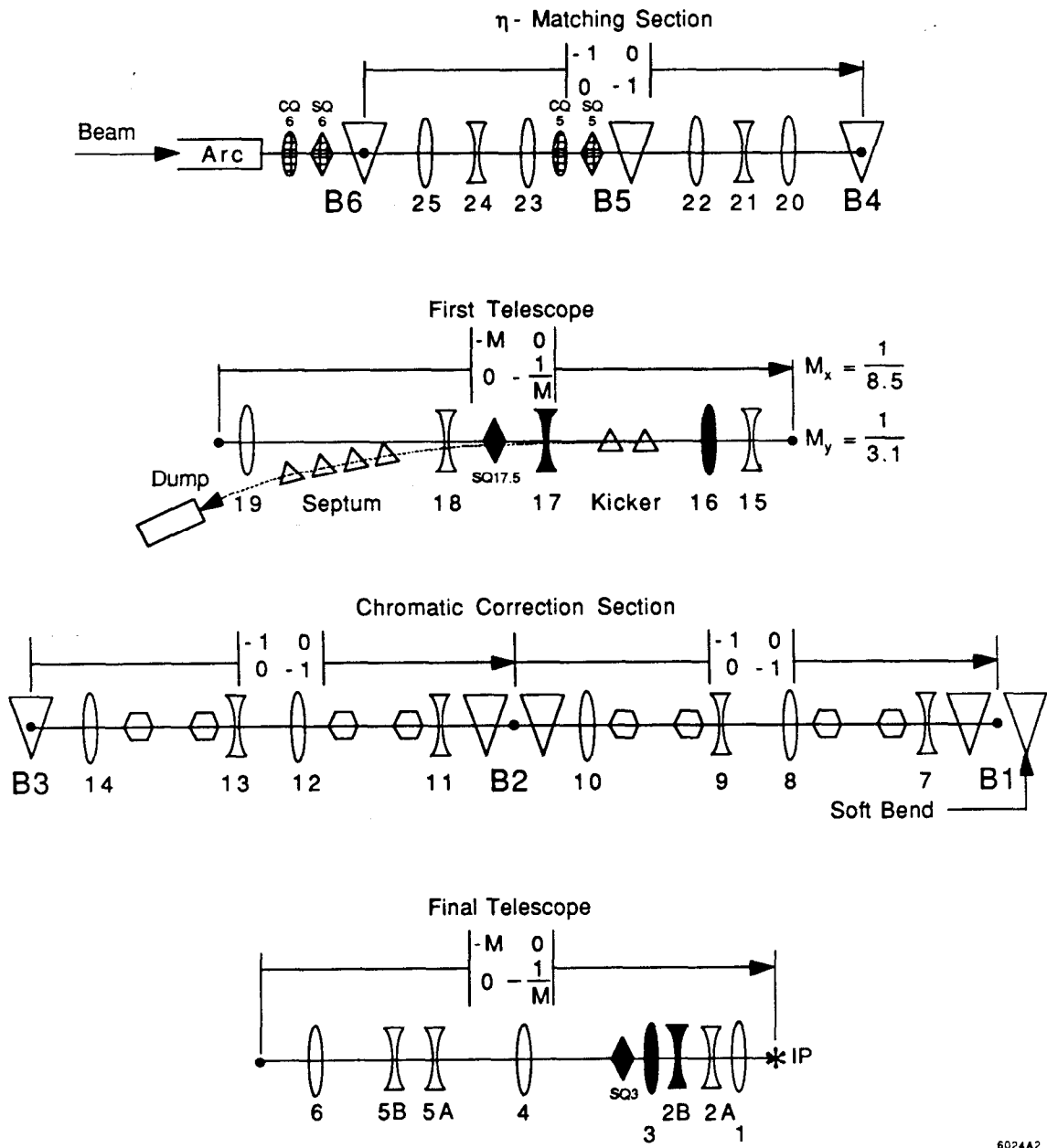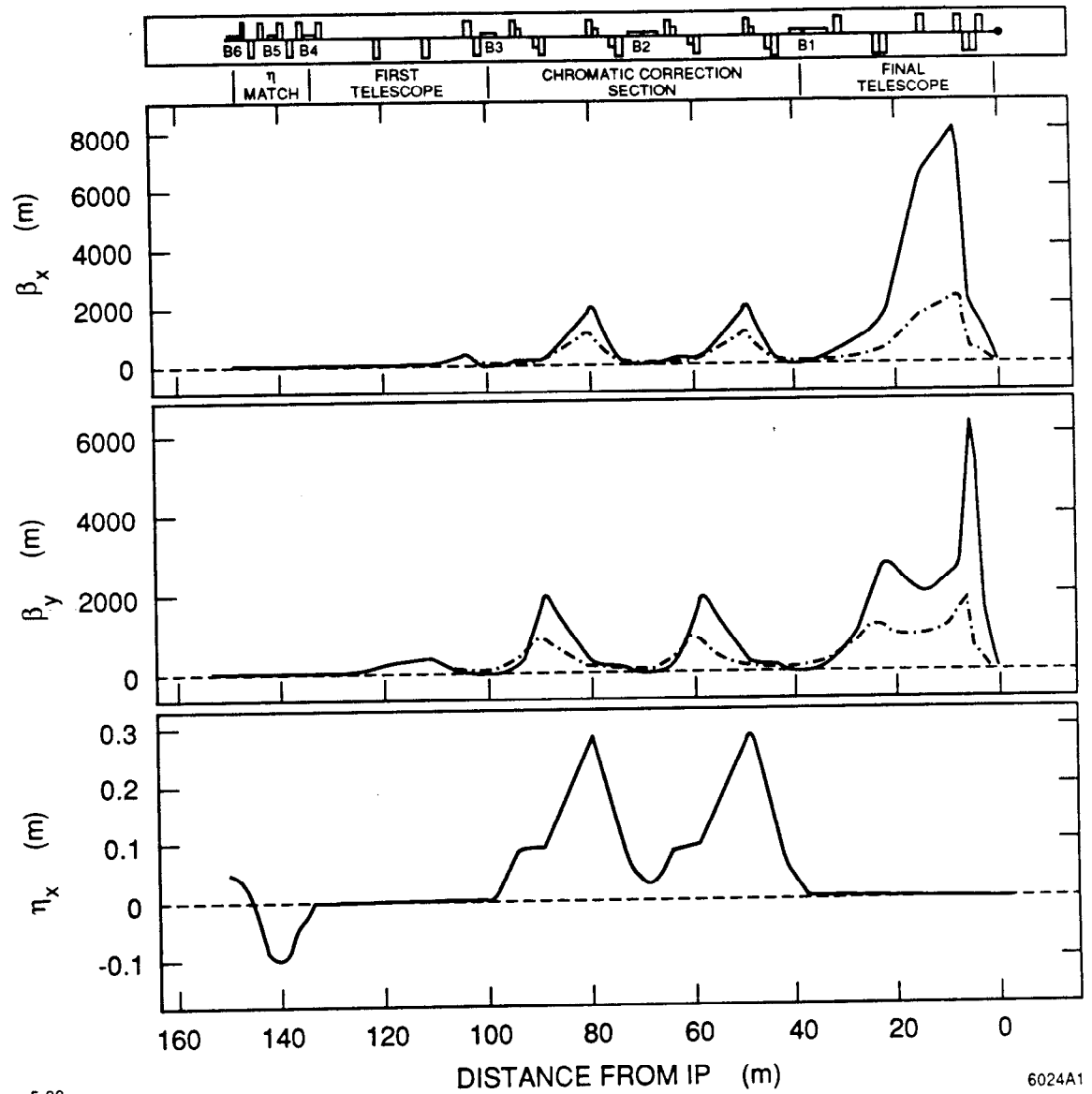
η - Matching Section

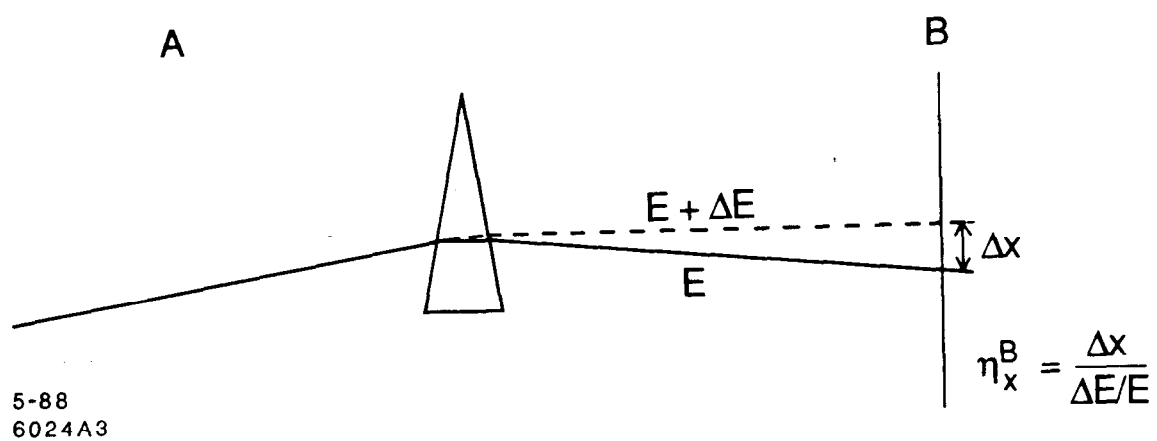$\begin{vmatrix} -1 & 0 \\ 0 & -1 \end{vmatrix}$

Beam → Arc

CQ 6   SQ 6   B6   25   24   23   CQ 5   SQ 5   B5   22   21   20   B4

First Telescope

$\begin{vmatrix} -M & 0 \\ 0 & -\frac{1}{M} \end{vmatrix}$

$M_x = \dfrac{1}{8.5}$

$M_y = \dfrac{1}{3.1}$

Dump   19   Septum   18   SQ17.5   17   Kicker   16   15

Chromatic Correction Section

$\begin{vmatrix} -1 & 0 \\ 0 & -1 \end{vmatrix}$ $\begin{vmatrix} -1 & 0 \\ 0 & -1 \end{vmatrix}$

B3   14   13   12   11   B2   10   9   8   7   B1

Soft Bend

Final Telescope

$\begin{vmatrix} -M & 0 \\ 0 & -\frac{1}{M} \end{vmatrix}$

* IP

6   5B   5A   4   SQ3   2B   2A   1
3

11-87   6024A2

Fig. 1

Fig. 2

A   B

$E + \Delta E$

Δx

E

$$\eta_x^B = \frac{\Delta x}{\Delta E/E}$$

5-88
6024A3

Fig. 3

BEFORE CORRECTION

AFTER CORRECTION

HORIZONTAL DISPERSION

η_x (mm)

ARC   η-MATCH
        AND
        FIRST
        TELESCOPE   CCS

—— DISPERSION MEASUREMENTS
--- DESIGN DESPERSION

DISTANCE ALONG BEAM LINE ⟶

η_x (mm)

VERTICAL DISPERSION
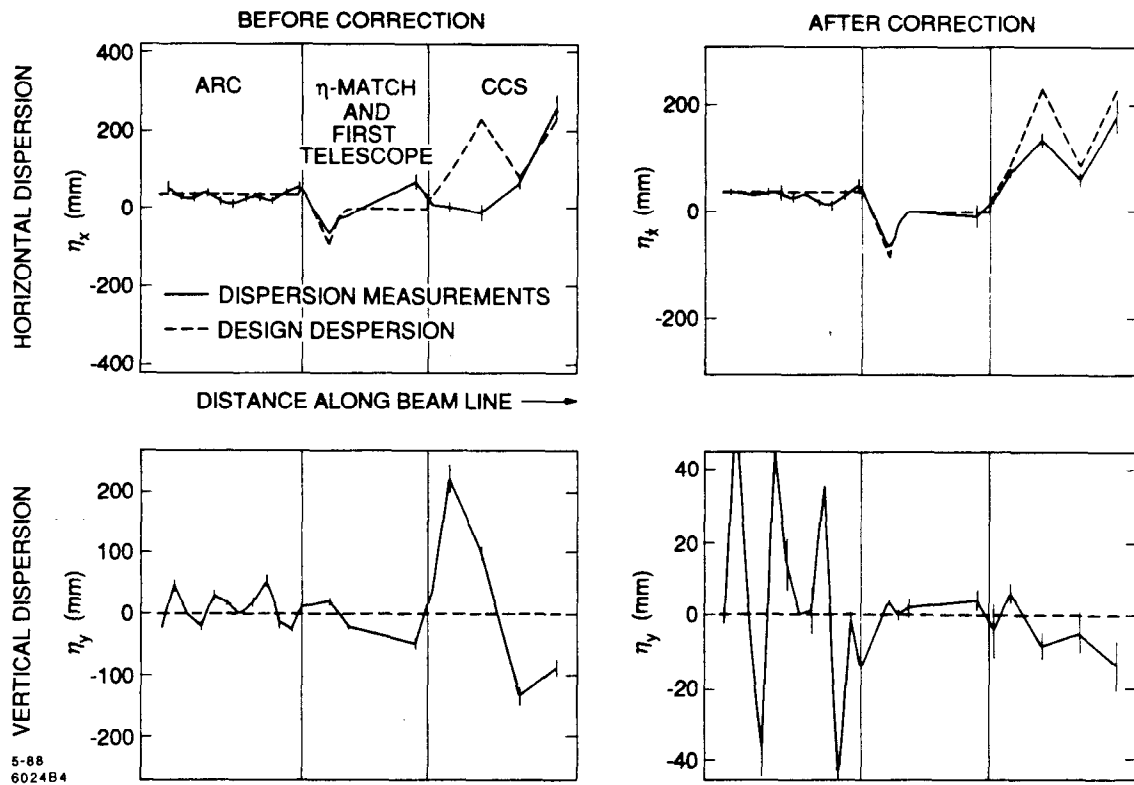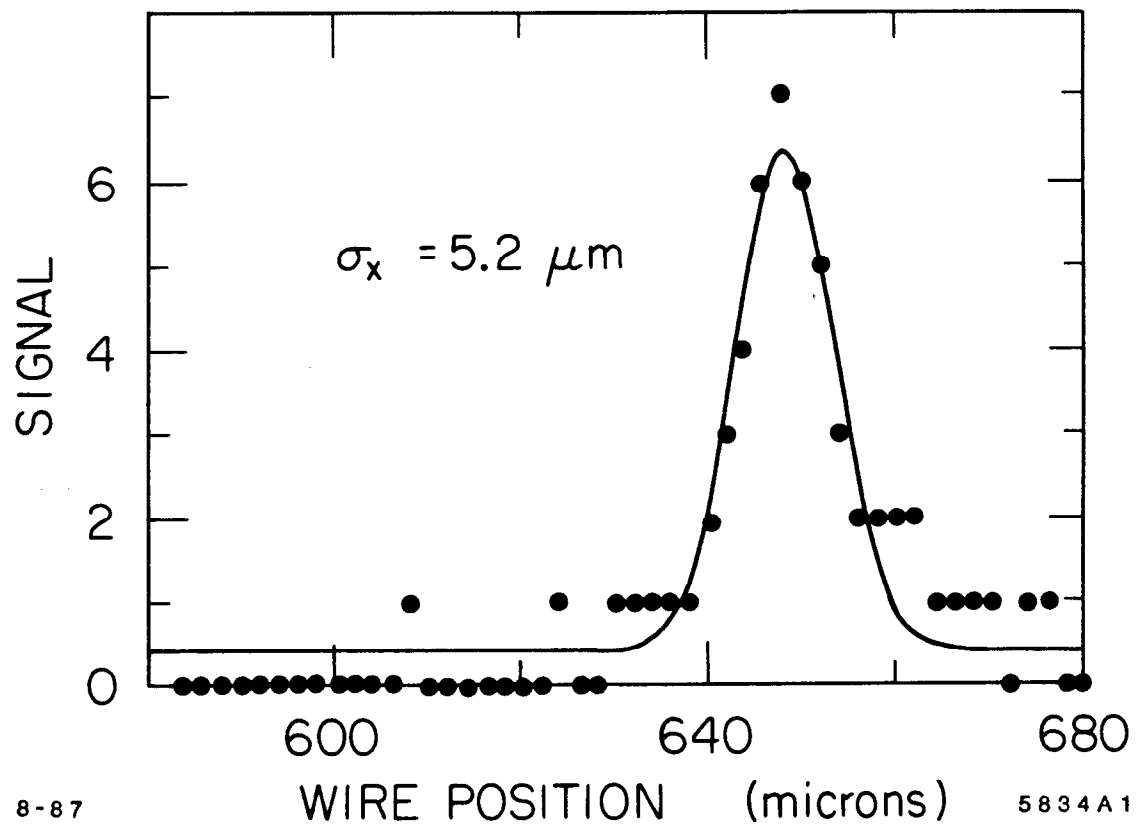
η_y (mm)

η_y (mm)

5-88
6024B4

Fig. 4

$\sigma_x = 5.2 \ \mu m$

SIGNAL

WIRE POSITION (microns)

8-87

5834A1

Fig. 5